Fast hybrid model for evaluating the scattering characteristics of target in complex environment

Fast hybrid model for evaluating the scattering characteristics of target in complex environment.

Paola Russo(1), Dihia Sidi Ahmed(2), Regis Guinvarc'h(2), and Laetitia Thirion(2)

(1) Department of Information Engineering, Università Politecnica delle Marche, 60131 Ancona, Italy https://www.univpm.it/
(2) SONDRA, CentraleSupélec, Université Paris-Saclay, F-91190 Gif-sur-Yvette, France

***Abstract*—This paper presents a tool that integrates an electromagnetic model based on physical optics (PO) for evaluating the reflection of large object, with a tool developed in a previous paper for characterizing the scattering characteristics of small and complex target. The aim is to provide a model for characterizing the interaction of the target with the surrounding environment. The model is fast and permits us to separate the contribution to the scattering characteristics of the target, due to the target itself and to the interaction with the external environment.**

I. Introduction

The need to identify small drones within urban contexts arises for reasons related to safety. The small size of the drones, the materials with which they are made, the fact that they typically fly at low altitudes pose problems in their identification, as the signal they reflect, based on radar monitoring, is quite low. The possibility of identifying and recognizing a drone in a complex environment such as, for example, the urban one requires first of all to have a rather precise knowledge of the object's scattering characteristics (RCS, micro-Doppler), but it is also necessary to have information on the influence of the environment on the target's response to the radar signal.

In literature there are several works that deal with analyzing the response of a drone to an electromagnetic signal, but to the best of our knowledge, no one has yet analyzed the interactions of the drone signal with the environment. Most extract the main features of the signal reflected by the drone using data from measurements, while others, few in reality, deal with creating electromagnetic models of individual parts or of the drone's interior, like the propellers as in [1] that uses an FDTD model to characterize them or [2] that proposed a very simplified model of the micro-Doppler response of the propeller.

In [3], we introduced a fast tool for characterizing the complete scattering behavior of complex target. In this paper, the tool is employed in conjunction with a physical optics model, which is used for simulating the reflection of electromagnetic fields from large objects, such as buildings in an urban environment, thereby developing a model of the interaction between the target and the environment.

The paper briefly summarizes the principal characteristics of the tool proposed in [3] and the physical optics (PO) algorithm. Subsequently, the development of the hybrid algorithm is detailed along with the preliminary results.

II. Generalized Scattering matrix

In [3] a fast computation of the electromagnetic scattering (EMS) characteristics of static or moving complex radar targets was proposed.

In general, for a complete description of the interaction of the incident and scattered waves and the targets, the information about the radar targets has to go beyond the scalar value of the radar cross-section (RCS). The RCS is the size of the target seen by the radar and is not always related to the physical size of the object. Moreover it depends only on the amplitude of the incident and scattered fields, so it cannot be used to obtain information on the microdoppler feature of the target and on his velocity and or trajectories. Our approach is to use a complex parameter that describes the complete scattering feature of the target, in the farfield. With this approach the scattered field is related to the incident field through a multidimensional matrix H:

$$\overrightarrow{E^s}(R_R,\theta,\phi) = H(\Theta,\Phi,\theta,\phi)\overrightarrow{E^i}(R_T,\Theta,\Phi)\frac{e^{-j\beta R_R}}{R_R} \quad (1)$$

where $\beta = \frac{2\pi}{\lambda}$ is the propagation constant, H is a [3 × 3] matrix, R_T is the radial coordinate of the target referenced to the transmitter position and R_R is the radial coordinate of the receiver referenced to the target position. This matrix depends on continuous variables $(\Theta,\Phi,\theta,\phi)$ so, in order to evaluate once and for all the scattering characteristic of the target, it is evaluated in specific directions (sampling directions) using a numerical tool or an experimental approach and when necessary the values for any incidence wave and any observation point is recovered through an interpolation procedure based on cardinal series. In our model we use the commercial electromagnetic software, CST Microwave Studio (CST MWS) [4] to evaluate the scattering of the target, at specific sampled directions. The method is developed using MATLAB.

As an example of reconstruction procedure, (2) provides the scattering matrix H elements for a generic scattering direction (θ,ϕ), due to an impinging wave coming from one of the sampled direction (Θ_i,Φ_{ij}). The specific element correspond to the x_p scattered component due to the x_q incident component, where x_p and x_q represent the generic cartesian coordinate.

$$h_{x_q}^{x_p}(\Theta_i, \Phi_{ij}, \theta, \phi) = \sum_{m=-M}^{M} \sum_{n=-N}^{N} h_{x_q}^{x_p}(\Theta_i, \Phi_{ij}, \theta_m, \phi_{mn})$$
$$\frac{sinc\Big((2N+1)(\frac{\phi-\phi_{mn}}{2})\Big)}{sinc\Big(\frac{\phi-\phi_{mn}}{2}\Big)} \frac{sinc\big((2M+1)(\frac{\theta-\theta_m}{2})\big)}{sinc\big(\frac{\theta-\theta_m}{2}\big)} \quad (2)$$

where $\theta_m = \frac{2\pi m}{2M+1}$ and $\phi_{mn} = \frac{2\pi n}{2N+1}$, with M and N the number of samples on the θ, ϕ spherical coordinates. More details on the complete reconstruction procedure can be found in [3].

III. Physical optics approach

The scattering field from large metallic object can be modelled using the physical optics (PO) approach ([5]). The PO approximations is based on the assumptions that the scattering field can be calculated evaluating the equivalent surface currents on the object, and assuming that the currents on the "shadow" region are negligibles. The PO model developed for our tool, is based on the discretization of the surface of the large reflecting object using triangular patches. The dimension of each patches need to be very small compared to the wavelength (their sides at least less then $\lambda/10$) so that the equivalent current on each subsurface can be considered uniform. On each subsurface the equivalent current is evaluated considering the local characteristic of the impinging wave. The interaction between patches is neglected, and this is another assumption related to the Physical Optics approximation. Figure 1 shows the geometry of the interaction of the impinging wave on one subsurface (red contour). In figure it can be seen the impinging field ray (R_i) and the scattered field ray (R_r) together with the normal to the subarea surface (n_p), the normal to the incident plane (light blue plane) (n_i) and its tangent unit vector (t_i).

$$\vec{J} = \hat{n}_p \times \left(\vec{H}_{\text{tan}}^{TE} + \vec{H}_{\text{tan}}^{TM}\right)$$
$$\vec{M} = \left(\vec{E}_{\text{tan}}^{TE} + \vec{E}_{\text{tan}}^{TM}\right) \times \hat{n}_p \quad (3)$$

The equivalent current on each subsurface are evaluated as in (3) where $\vec{H}_{\text{tan}}^{TE}, \vec{H}_{\text{tan}}^{TM}, \vec{E}_{\text{tan}}^{TE}, \vec{E}_{\text{tan}}^{TM}$ represent the total fields for the usual two polarizations TE and TM of an oblique incident problem between two indefinite media. The total field for each polarization is evaluated considering the proper reflection coefficient as, for example, in (4)

$$\vec{E}_{\text{tan}}^{TE} = (1 + \rho^{TE})\vec{E}_{\text{tan}}^{iTE} \quad (4)$$

Once the equivalent current are evaluated the electromagnetic fields scattered by the object are calculated from the usual vector potential $\vec{A}$ and $\vec{F}$. As an example in (5) the evaluation of the scattered electric field is reported.

$$\vec{E}_n^s = \frac{\nabla\nabla \cdot \vec{A}}{j2\pi f \varepsilon\mu} - j2\pi f \vec{A} - \frac{1}{\varepsilon}\nabla \times \vec{F} \quad (5)$$

More details on the general procedure for the scattering of a real object can be found in [6].

The subdivision of the object surface into small subarea permits to work in far-field condition for each electric and magnetic field scattered by the equivalent sources. In this way also a near field problem can be treated in a simple way. The scattered electric and magnetic fields are superposed directly at the receiver position.

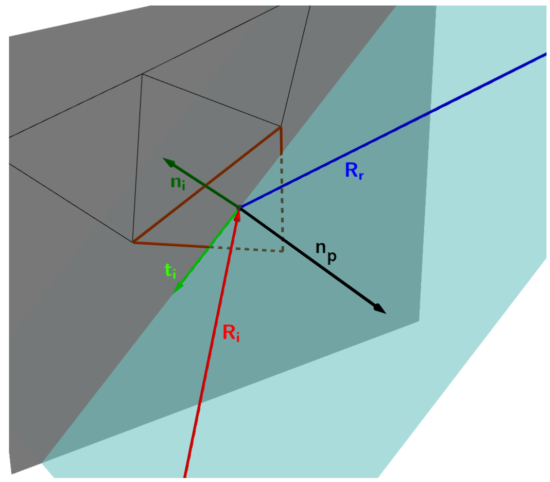

Fig. 1. Details of the interaction between impinging wave and the scattering object surface

IV. Hybrid model

The scenario to investigate is a drone operating within an urban environment. The different dimension of the scattering object leads to the use of the most proper modellization. To be more clear. A large scattering object, like a building in urban area, can be modeled using the PO approximation, whereas a small object, moreover complex, like a drone can be modelled with model proposed in section II. If the two types of object are present in the scattering problem an hybrid approach can be used. In order to present the hybrid approach the scenario can be simplified: the drone is replaced by a sphere, and a wall represents the urban environment. This simplified scenario is sufficient to introduce multiple interactions and additional responses.

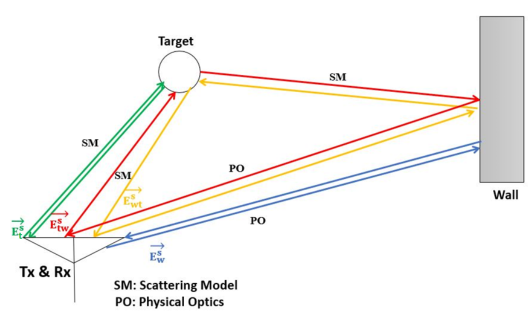

Fig. 2. The scenarios covered by the Hybrid Model: Monostatic Case.

Figure 2 shows the four main components that contribute to the received signal in the monostatic case, together with the type of model to be adopted for each contribution (Scattering matrix (SM) and PO). The received electric field can be written as:

$$\vec{E}^s_{total} = \vec{E}^s_t + \vec{E}^s_w + \vec{E}^s_{tw} + \vec{E}^s_{wt} \quad (6)$$

We will delve into the calculation process for each contribution, highlighting the steps in assessing their impact on the overall field received at the receiver.

1) The direct scattering of electromagnetic waves by the target: To evaluate the field scattered directly from the target denoted $\vec{E}^s_t$, we utilize the model presented in Section II. The method allows us to assess the scattered field at any point in space that is illuminated by an antenna positioned at any location. Considering the geometry represented in Figure 2, we want to calculate the field radiated by the transmitting antenna Tx and scattered by the target towards the receiving antenna Rx. With respect to a spherical reference system centered on the target, the Tx antenna is located at (R_{T_x}, Θ, Φ), and the Rx antenna is located at (R_{R_x}, θ, ϕ).

The field incident $\overrightarrow{E^i}$ on the target is given by:

$$\overrightarrow{E^i} = \sqrt{\frac{2\eta P_{Tx} G_{Tx}(\Theta,\Phi)}{4\pi R^2_{T_x}}} e^{-j\beta R_{T_x}} \hat{\mathbf{e}} \quad (7)$$

Where:

- η is the free space wave impedance,
- P_{Tx} is the radiated power,
- $G_{Tx}(\Theta,\Phi)$ is the transmitting antenna gain in the (Θ,Φ) direction,
- R_{T_x} is the distance from the transmitting antenna to the target,
- β is the wave number, also noted $k = \frac{2\pi}{\lambda}$,
- $\hat{\mathbf{e}}$ is the unit vector indicating the polarization direction of the electric field.

The field scattered by the target at the receiving antenna can be expressed as in Eq. 1.

2) The direct scattering of electromagnetic waves by the wall : Using the PO approach presented in Section III, the building wall can be divided into i sub-areas, with $i \in 1, N$ characterized by their proper reflection coefficients as the incidence and scattering angles locally change. Electric and magnetic currents can be calculated from these sub-areas, and their radiation will contribute to the field denoted as $\overrightarrow{E^s_w}$ and received by Rx. We will obtain $\overrightarrow{E^s_w} = \sum_{i=1}^N \overrightarrow{E^s_{w_i}}$, with $\overrightarrow{E^s_{w_i}}$ that depends on the field incident on the cell i, with the incident angles $(\Theta_{w_i}, \Phi_{w_i})$ with a distance R_{TxW_i} between this i^{th} cell and the transmitter. The scattering is computed in the direction of the receiver at a distance R_{RxW_i}, with the scattering angles $(\theta_{w_i}, \phi_{w_i})$. To compute this contribution, we directly used the code developed in [6].

3) The electromagnetic waves reflected by the wall due to the target's illumination: Similarly, as in the previous component, we will use the PO-based code for evaluating the reflection from the wall. For the impinging wave on each cell i of the wall due to the target, we calculate the field scattered by the target, using the H matrix of the target. After, we compute the field scattered by each wall cell toward the receiver. Finally, the sum of the contributions of all the N cells produces $\vec{E}^s_{tw}$.

4) The electromagnetic waves reflected by the target due to the wall's illumination: In this case, first the reflected field $\overrightarrow{E^r}_{w_i}$, due to the direct illumination of each subarea of the wall from the antenna is evaluated with PO model. This field impinges on the target and it is then scattered in every direction. We compute the contribution $\vec{E}^s_{wt_i}$ of each scattering field towards the receiver using the generalized scattering matrix approach.

Finally $\vec{E}^s_{wt} = \sum_{i=1}^N \vec{E}^s_{wt_i}$. In order to maintain the assumption of farfield the field reflected by each subarea $\overrightarrow{E^r}_{w_i}$ is used as illumination for the target and the summation of each contribution is done only on the receiver.

V. Results

The model was applied to a simplified geometry, in order to analyse all the contribution presented in the previous section. Figure 3 illustrates the configuration setup on Matlab using the hybrid model. A 20 cm perfectly conducting (PEC) sphere was positioned in front of a PEC wall.

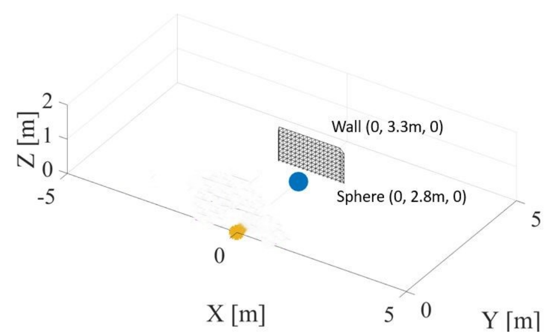

Fig. 3. Simulation of the Sphere in the Presence of the Wall using SM model

The wall is made of PEC and it has a height extending along the z-axis of 2 m, a length along the x-axis spanning 2 m, and a thickness along the y-axis measuring 2 cm. This wall is positioned at a distance of 50 cm from the center of the PEC sphere.

This configuration assumes the use of a horizontally polarized plane wave with incident angles of ($\Theta = 90°$, $\Phi = 270°$) and a frequency of 500 MHz. The sphere is moving from the initial position toward the antenna at a speed of 7.5 m/s. To perform the Doppler analysis, its position is sampled every 625 μs, corresponding to a displacement of 4.5 mm between consecutive positions. To describe the whole path (1.5m) , 321 different positions are analyzed.

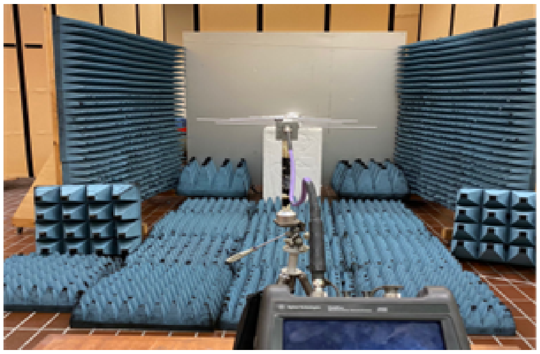

Fig. 4. Measurement set-up

In order to validate the model the same configuration was also measured in our lab at Università Politecnica delle Marche. (see Fig. 4).

Figure 5 shows the spectrogram measured. Whereas Fig. 6 the simulated one. In both cases the static clutter was removed. The two spectrograms are very similar to each other even if with some differences. It can be seen from the spectrogram that the amplitude of the signal increase as expected when the sphere moves towards the receiver. However there is a stationary pattern both in the measurement and in the simulation due to the reflection effect of the field scattered by the sphere on the static object. In the measurement results this effect is more pronounced and the spectrogram is more noisy. Probably this is due to the non-anechoic environment of our lab so that the reflection comes not only from the wall but also from other objects.

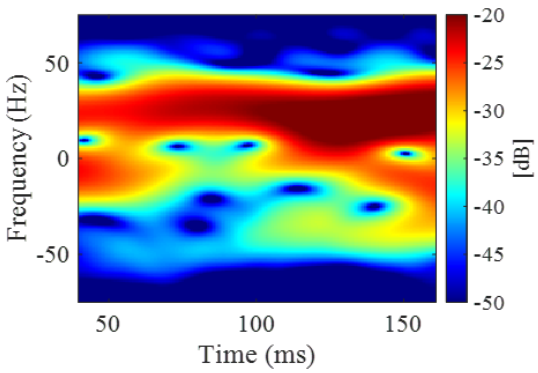

Fig. 5. Spectrogram of the measured receive field after removing the clutter

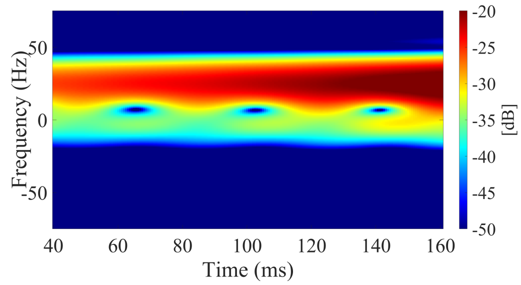

Fig. 6. Spectrogram of the simulated received field removing the wall contribution

Regarding the simulation time, once the H matrix of the sphere is known each contribution for all the 321 positions of the sphere needs less then 30s. A very fast simulation if compared to 30 min necessary for each position of the sphere using a full wave simulation tool like CST.

VI. Conclusion

This paper introduces a tool that combines an electromagnetic model based on physical optics (PO) to evaluate the reflection of large objects with a previously developed tool for characterizing the scattering characteristics of small and complex targets. The goal is to create a model that describes how a target interacts with its surrounding environment while in motion. This tool is crucial for computing the time-Doppler signature of a UAV, for example. In this study, we applied our code to a simple scenario involving a metallic sphere moving near a large metallic plane, which we are able to replicate in a semi-anechoic chamber. The promising results from this configuration pave the way for more intricate tests and further analyses.

References

[1] M. Ritchie, F. Fioranelli, H. Griffiths, and B. Torvik, “Micro-drone rcs analysis,” in *2015 IEEE Radar Conference*. Johannesburg, South Africa: IEEE, 2015.

[2] Y. Cai, O. Krasnov, and A. Yarovoy, “Simulation of radar micro-doppler patterns for multi-propeller drones,” in *2019 International Radar Conference (RADAR)*, Toulon, France, 2019, pp. 1–5.

[3] D. S. Ahmed, P. Russo, G. Cerri, L. T. Lefèvre, R. Guinvarc’h, and G. Manfredi, “A numerically efficient method for predicting the scattering characteristics of complex moving targets,” *IEEE Transactions on Antennas and Propagation*, vol. 71, no. 1, pp. 910–920, Jan. 2023.

[4] “CST software,” https://www.3ds.com/fr/produits-et-services/simulia/produits/cst-studio-suite.

[5] E. F. Knott, J. F. Schaeffer, and M. T. Tulley, *Radar cross section*. SciTech Publishing, 2004.

[6] G. Manfredi, P. Russo, A. De Leo, and G. Cerri, “Efficient simulation tool to characterize the radar cross section of a pedestrian in near field,” *Progress In Electromagnetics Research C*, vol. 100, p. 145 – 159, 2020.